doi.org/10.36721/PJPS.2024.37.2.SP.463-473.1

Anti-inflammatory effects of steroidal alkaloids of *Solanum lyratum* Thunb.

Lijie Yang[1], Yiming Yang[1], Qi Wang[1], Hongtian Fei[2], Rui Fei[1,3]*, Yajuan Xu[4]* and Chunmei Zhang[1]*

[1]Department of Cell Biology, College of Basic Medical Science, Jilin University, Changchun, Jilin, China
[2]Department of Pharmacology, College of Basic Medical Sciences, Jilin University, Changchun, Jilin, China
[3]Key Laboratory of Lymphatic Surgery Jilin Province, Jilin University, Changchun, Jilin, China
[4]Key Laboratory of Effective Substances of Traditional Chinese Medicine Jilin Province, Jilin Academy of Chinese Medicine Sciences, Chang Chun, Jilin, China

Abstract: *Solanum lyratum* Thunb., a traditional Chinese herbal medicine, has a promising background. However, the anti-inflammatory effects of its component steroid alkaloid have not been explored. In this study, animal and cell experiments were performed to investigate the anti-inflammatory effects and mechanism of action of *Solanum lyratum* Thunb steroid alkaloid (SLTSA), in order to provide evidence for its potential utilization. SLTSA effectively inhibited ear swelling and acute abdominal inflammation of mice. We observed concentration-dependent inhibition of pro-inflammatory cytokines by SLTSA, as confirmed by the ELISA and RT-qPCR results. Flow cytometry, immunofluorescence and RT-qPCR analyses revealed that SLTSA suppressed TLR4 expression. Western blot results indicated that SLTSA inhibited the activation of the TLR4/MyD88/NF-κB signaling pathway. Our study demonstrated that SLTSA possesses anti-inflammatory properties.

Keywords: *Solanum lyratum* Thunb., steroidal alkaloid, anti-inflammatory, inflammatory cytokines, TLR4

INTRODUCTION

Inflammation is an important immune response of the body. However, once this kind of intricate response is overdone, it may cause more serious damage to the organism or disease deterioration (Tasneem *et al.*, 2019). Even though medications are available to treat inflammation, there are still significant side effects, including allergic reactions and the development of drug resistance (Christaki *et al.*, 2020; Allgaier *et al.*, 2023). Therefore, the exploitation of safer anti-inflammatory drugs is necessary.

Solanum lyratum Thunb (SLT) called "Baiying" in Chinese, is a traditional Chinese herbal medicine from the *Solanaceae* family and is widely used in clinical practice (Liu *et al.*, 2023). Its extracts exert anti-cancer, anti-inflammation, anti-microbial, anti-allergy and anti-oxidation activities (Zhao *et al.*, 2022; Liang *et al.*, 2022). Especially in antitumor applications, it has been reported that SLT extracts could inhibit the proliferation of ovarian cancer cell and other cancer cells (Chen *et al.*, 2020; Zhang *et al.*, 2021). The active components of SLT, such as solalyratins, have shown anti-inflammatory activities because of the inhibition of beta-glucuronidase release in rat polymorphonuclear neutrophils (Zhang *et al.*, 2010), Zou *et al.* found that formulation of SLT can also ameliorates thromboangiitis obliterans by inhibiting the activation of ERK, JNK, p38-MAPK and HMGB1/RAGE/NF-κB signaling pathways (Zou *et al.*, 2022). It can be seen that SLT has potential anti-inflammatory application prospects.

Literature reviews have shown that steroidal alkaloids have amphiphilic molecular characteristics and can regulate the expression of genes or proteins inside cells, thus, steroidal alkaloids from various herbs are widely used in anti-cancer and anti-inflammatory research (Li *et al.*, 2021; Zhou *et al.*, 2023; Li *et al.*, 2023), for example, the steroidal alkaloid isolated from *Solanum nigrum* Linn. possessed a potent anti-inflammatory property in RAW264.7 macrophages and animal models of inflammation, including xylene-induced ear edema formation (Zhao *et al.*, 2018). Besides, the jervine, a sterodial alkaloid from Veratrum album, can inhibit inflammatory biomarkers such as TNF-α and IL-1β in rat serum to exert anti-inflammatory effects (Dumlu *et al.*, 2019). As its active component, SLTSA is a basic nitrogen compound, and its structure has been clearly defined in our previous study (fig. 1) (Xu *et al.*, 2018), however, its anti-inflammatory effects have yet to be elucidated.

TLR4 as a pattern recognition receptor, was the first member of the Toll-like receptor family to be identified and is an important anti-inflammation target (Tam *et al.*, 2023). Many alkaloid compounds isolated from Chinese herbal have been found to inhibit the inflammatory response by inhibiting the expression of TLR4 (Zhang *et al.*, 2019; Shen *et al.*, 2021; Geng *et al.*, 2021; Xu *et al.*, 2022). Previous studies have shown that TLR4 can be stimulated by lipopolysaccharide (LPS) to induce

**Corresponding authors:* e-mail: Y18844115611@163.com

cascades (Ciesielska *et al.*, 2021), triggering MyD88-dependent or MyD88-independent signaling pathways (Jin *et al.*, 2022), among which the TLR4/MyD88/NF-κB signaling pathway is more crucial and occurs earlier (Li *et al.*, 2022). At the end of this signaling pathway, NF-κB translocates to the nucleus to initiate gene expression (Mohammad *et al.*, 2020). Excessive activation of TLR4 can cause inflammation in various organs and aggravate functional injury in the body (Wang *et al.*, 2023). Studies have confirmed that the TLR4/MyD88/NF-κB pathway is involved in the development and progression of immunoglobulin-mediated nephropathy, leading to renal impairment (Zhang *et al.*, 2020). TLR4 plays a central role in the inflammatory process and has become a potential target for therapeutic intervention (Bowman *et al.*, 2017). Therefore, in-depth exploration of this signaling pathway is important for elucidating the anti-inflammatory mechanism of SLTSA.

This study aimed to explore the anti-inflammatory effects of SLTSA at the animal, cellular, and molecular levels, as well as to demonstrate the role of SLTSA in the TLR4/MyD88/NF-κB signaling pathway, to investigate the anti-inflammatory mechanism of SLTSA and to provide more evidence for the further development of the anti-inflammatory value of SLTSA for the effective control of inflammation.

MATERIALS AND METHODS

Animals and cell line

Six- to eight-week-old male BALB/c mice (20±2 g) were purchased from Changchunshi Yisi Experimental Animals Technology Limited. Mice were housed in the Jilin University Animal Experimental Center of Basic Medical Sciences under controlled temperature (22-24 °C) and light (14h light/10h dark), with water and food provided ad libitum.

RAW264.7 cells were purchased from the Cell Bank of the Shanghai Branch of the Chinese Academy of Sciences and incubated at 37°C in a 5% CO_2 incubator.

Construction of mice ear edema model

The animal study protocol was approved by the Ethics Committee of the Ethics Committee of College of Basic Medical Sciences, Jilin University (AP# 2024-289). Sixty mice were randomly divided into six groups, each with ten mice: diluent control group (Mock), model group (Model), positive dexamethasone control group (DXM), and three drug concentration groups of low, medium and high SLTSA. Weighed 4 g SLTSA powder, was dissolved in 1ml DMSO, diluted into storage solutions with concentrations of 0.5, 2 and 4mg/ml and all drugs were sterilized through a 0.22μm filter. The mice in the positive control group were injected with dexamethasone (1.25mg/kg) in the tail vein, and the other group mice were injected SLTSA storage solutions 100μl in the tail vein once per day for 7 days. On the seventh day, 50μl of xylene was applied to the same part of the right ear only for each mouse except for the Mock control group, and the left ear was used as the control. After 1.5h, mice were euthanized by carbon dioxide according to the "standard procedure for carbon dioxide Euthanasia of Laboratory Animals". Their ear sections were immediately taken from both ears of mice at the same location with a punch and weighed on an analytical balance and the ear swelling rate was calculated according to the following formula:

Ear swelling rate (%) = (right ear weight - left ear weight)/left ear weight × 100%

The right ear of each mouse was fixed in 4% paraformaldehyde solution for 48h for immersion and fixation, embedded in paraffin, and cut into 5μm thick sections. Sections were stained with hematoxylin and eosin (HE) according to a standard procedure for the assessment of histopathological changes.

Construction of mice acute abdominal inflammation model

Sixty mice were randomly divided into six groups, each with ten mice, mice were injected with 1ml 3% thioglycolate broth intraperitoneally to perform a model of acute abdominal inflammation and five minutes later, the Mock and Model group mice were injected with PBS 100μl in the tail vein, the positive control group mice were injected with dexamethasone (1.25mg/kg) in the tail vein, and the other group mice were injected SLTSA storage solutions 100μl in the tail vein. Three hours later, the mice were anesthetized, and blood was collected from the eyes of the mice to detect the release of inflammatory cytokines using ELISA kits.

Mice were euthanized by carbon dioxide and dissected immediately after taking blood from the eyes, and the abdominal cavity was rinsed with 1 ml of saline and then diluted 10 times to count the leukocytes under a microscope (Motic, AE2000).

CCK8

RAW264.7 cells were cultured in 96-well plates. At 80% cell confluence, LPS (working concentration 1μg/ml) was added to each group of RAW264.7 cells for 12h, then the cells were received the following treatments: low (5 μg/ml), medium (20μg/ml) and high (40μg/ml) SLTSA concentration. After 24h, 100μl of medium and 10μl of CCK8 reagent were added to each well under light-proof conditions. After continued incubation at 37°C for 1h, the OD value was detected at 450nm on the enzyme analyzer.

ELISA

Blood from the mice was centrifuged at 3000 rpm for 20 min (4°C). The release of IL-1β, IL-6 and TNF-α inflammatory cytokines in the serum of each group of

mice was measured according to the instructions of ELISA kits.

RAW264.7 cells were cultured in 96-well plates. At 80% cell confluence, LPS was added to cells for 12h to perform a cell inflammation model, excluding the Mock group, then DXM (working concentration 1μM) and different concentrations of SLTSA were added separately. After incubation for 24h, 100μl of supernatant from each well was pipetted into EP tubes and centrifuged at 1500 rpm for 10 min (4°C) and then the cells were tested for secretion of IL-1β, IL-6 and TNF-α inflammatory cytokines according to the instructions of ELISA kits.

Flow Cytometry

RAW264.7 cells were cultured in 6-well plates. LPS was added to cells for 12h excluding the Mock group, then DXM and different concentrations of SLTSA were added separately. After incubation for 24h, the cells were collected in Ep tubes and fixed with 4% paraformaldehyde for 30 min (RT) separately. They were then blocked with 10% goat serum for 30 min (RT), labeled with a TLR4 antibody (1:100) for 6h (4°C) and labeled with the fluorescent secondary antibody (1:200) for 2h (RT, dark). Finally, the light signal of these cells near the wavelength of 575 nm was detected.

RT–qPCR

RAW264.7 cells were cultured in 6-well plates. At 80% cell confluence, LPS was added to cells for 12h excluding the Mock group, then DXM and different concentrations of SLTSA were added separately. After incubation for 24 h, RT-qPCR was performed on whole-cell extracts using primers for IL-1β, IL-6, TNF-α and TLR4. Data were analyzed using the ΔΔCT relative quantification method. Primer sequences are shown in table 1.

Cellular immunofluorescence

After RAW264.7 cells were inoculated in a 24-well plate, 4% paraformaldehyde was added to the plate for 30 min (RT), and 0.1% Triton X-100 was used to treat for 15 min (RT). Then, the cells were blocked with 10% goat serum for 30 min (RT) and labeled with a TLR4 antibody (1:100) overnight (4°C). Finally, these cells were labeled again with a fluorescent antibody (1:200) for 2h (RT, dark) and incubated with DAPI dye for 30 min. After the nuclei were stained (RT, dark), the cells were photographed and observed under a microscope (Olympus, IX71).

Western blot

Total cellular protein was extracted, and 20 μg of protein was added to each polyacrylamide gel well. After the protein was separated by SDS-PAGE electrophoresis, it was transferred to a PVDF membrane. Then, the PVDF membrane was blocked with 5% skim milk for 2 h and incubated with TLR4, MyD88, NF-κB (p65) and NF-κB (pp65) antibodies overnight (4°C) followed by incubation with HRP antibody for 2h (RT). Finally, ECL was used to visualize the PVDF membrane and the grayscale values of each band were analyzed by Image J software.

STATISTICAL ANALYSIS

All data were obtained from three experiments and presented as the mean ± standard deviation. GraphPad Prism software (version 9.0) was used to perform statistical analyses. Statistical analysis was carried out using the t-test to assess the significance of outcomes between groups. A significance level set at $p<0.05$ represented a statistically significant difference between groups.

RESULTS

Inhibition of ear swelling in mice by SLTSA

To investigate the anti-inflammatory effect of SLTSA, we performed the ear edema model in mice. Our results showed that compared with the Model group, the ear swelling rate of mice treated with SLTSA decreased with increasing concentration ($*p<0.05$, $**p<0.01$ and $***p<0.001$), with the most significant difference in the high concentration group, and the difference was statistically significant compared with the Model group ($**p<0.01$, $***p<0.001$) (fig. 2 A, table 2).

The HE staining results showed that the thickness of the dermis between the ear tissues of the mice in the Mock control group was normal, transverse muscle fibers with clear lines and intact borders were visible, and the blood vessels were not inflated and hyperemic. The thickness of the dermis of the ear tissues of the mice in the model group was increased by more than three times, the transverse muscle fibers were broken, the borders were blurred and discrete and the blood vessels were obviously dilated and hyperemic. After treatment with DXM, the edema of the ear tissues was restored. After treatment with SLTSA at low concentrations, although the hyperemia of mouse ear tissue was somewhat reduced compared to that of the model group, the swelling did not decrease significantly and there was chronic inflammatory cell infiltration. After treatment with SLTSA at a medium concentration, although there was still a small amount of inflammatory cell infiltration compared with the model group, the hyperemia of mouse ear tissue was almost invisible, and the thickness of ear tissue also decreased to a certain extent compared with the model group. After treatment with SLTSA at a high concentration, the thickness of the mouse ear tissue basically tended to a normal level, the transverse muscle rupture caused by edema was obviously modified, and blood vessel dilation and hyperemia were not obvious (fig. 2 B-D, table 2). These results showed that SLTSA can inhibit ear swelling in mice.

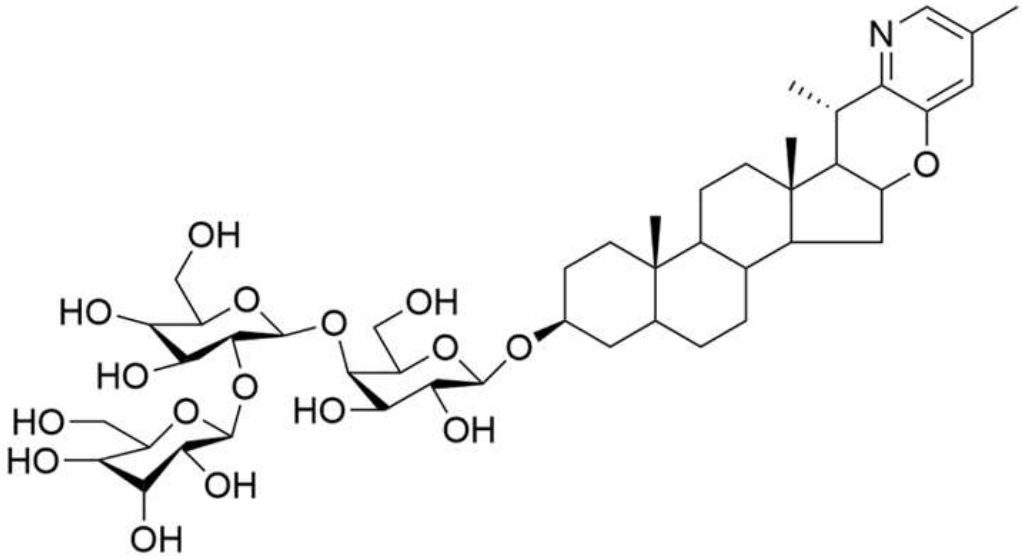

Fig. 1: Chemical structure of SLTSA

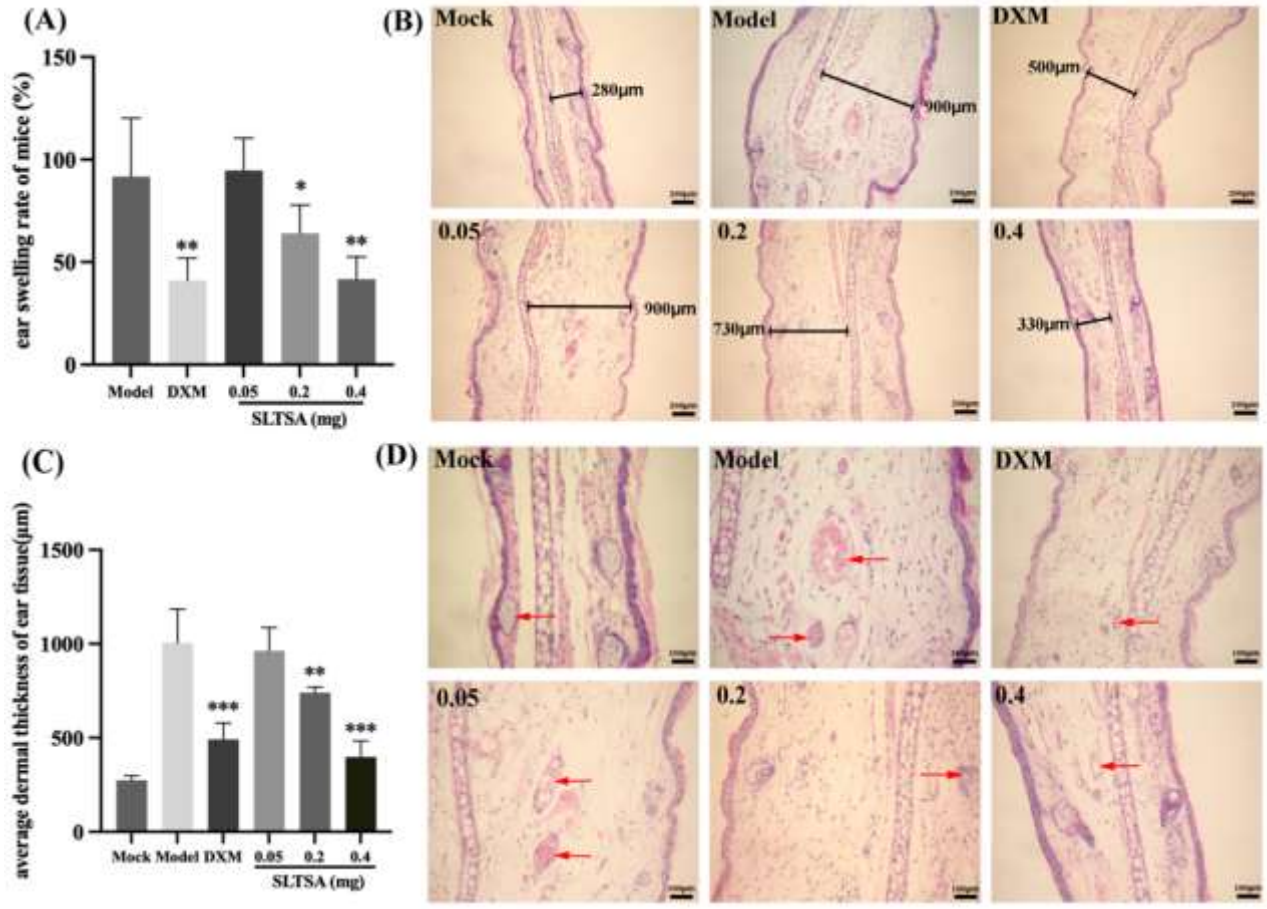

Fig. 2: Effect of SLTSA on ear edema model mice. (A) Ear swelling rate of mice. (B) HE staining of ear tissues (×100), black bidirectional arrows and (C) show the average dermal thickness of ear tissues. Scale bar = 200 μm (D) HE staining of ear tissues (×200), red arrows show blood vessels. Scale bar = 100 μm Mock: diluent control group; Model: model group; DXM: dexamethasone control group; 0.05, 0.2, 0.4: low, medium, high dose of SLTSA, respectively. *p<0.05, **p<0.01 and ***p<0.001 *vs.* the Model group.

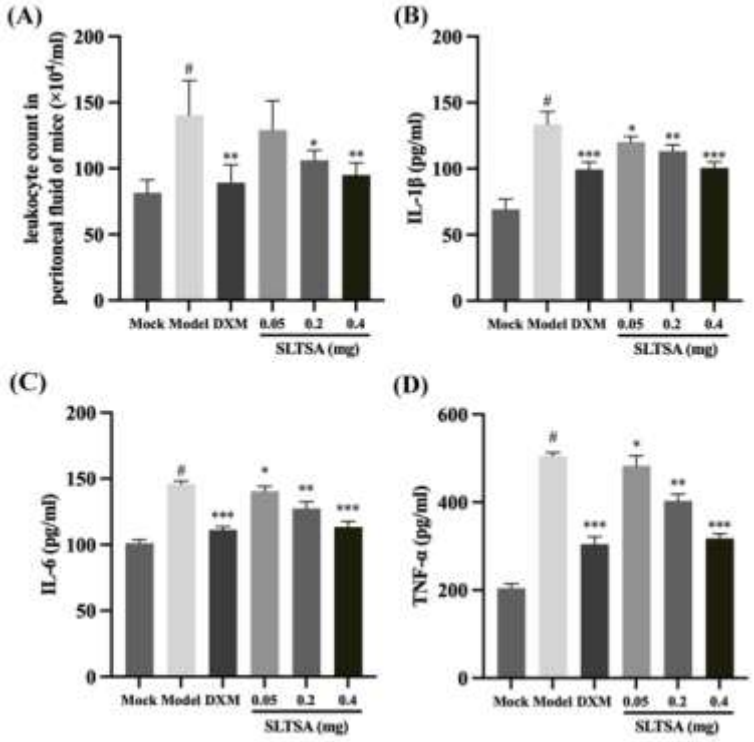

Fig. 3: Effects of SLTSA on acute abdominal inflammation in mice. (A) Abdominal leukocyte count in mice; (B-D) ELISA results of serum IL-1β, IL-6 and TNF-α cytokines. Mock: diluent control group; Model: model group; DXM: dexamethasone control group; 0.05, 0.2, 0.4: low, medium, high dose of SLTSA, respectively. $^{\#}p<0.001$ *vs.* Mock group, $^{*}p<0.05$, $^{**}p<0.01$ and $^{***}p<0.001$ *vs.* Model group.

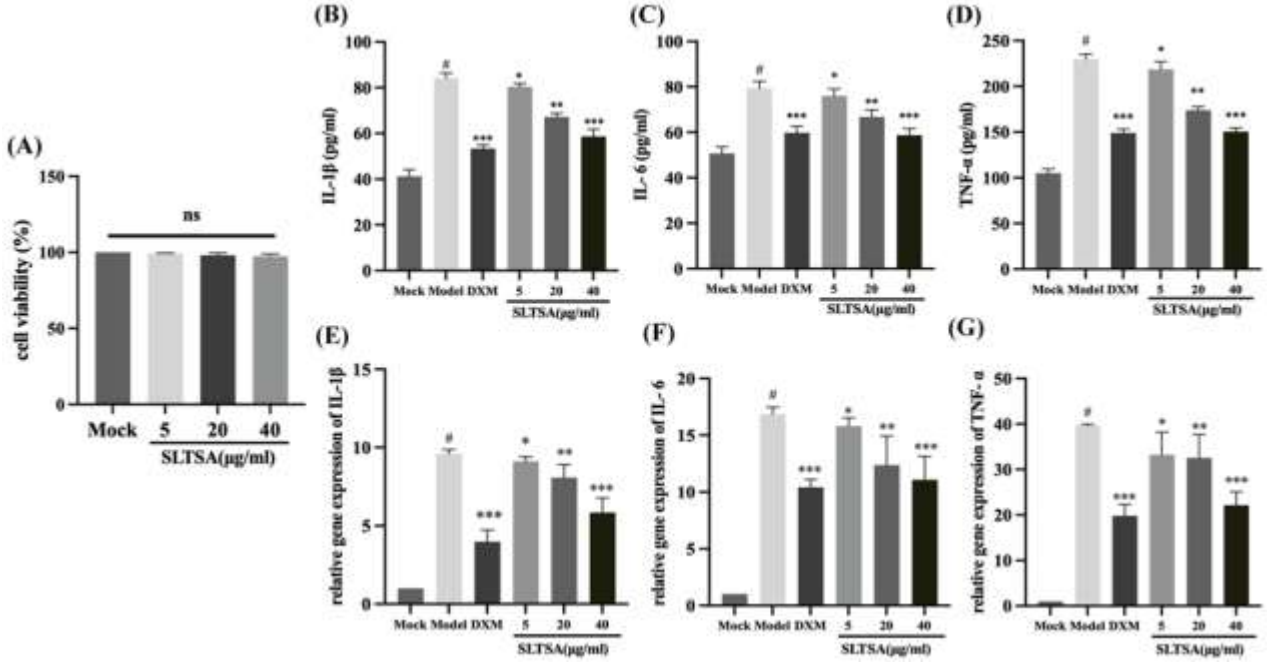

Fig. 4: Effect of SLTSA on cell viability and the expression of IL-1β, IL-6 and TNF-α cytokines. (A) CCK8 assay results. (B-D) ELISA results of SLTSA on the secretion of cellular IL-1β, IL-6 and TNF-α cytokines. (E-G) RT-qPCR results of SLTSA on the gene expression of IL-1β, IL-6 and TNF-α. Mock: diluent control group; Model: model group; DXM: dexamethasone control group; 5, 20, 40: three treatment groups with low, medium and high concentrations of SLTSA, respectively. ns: $p>0.05$ vs. each SLTSA group; $\#p<0.001$ vs. the Mock group, $*p<0.05$, $**p<0.01$ and $***p<0.001$ vs. the Model group.

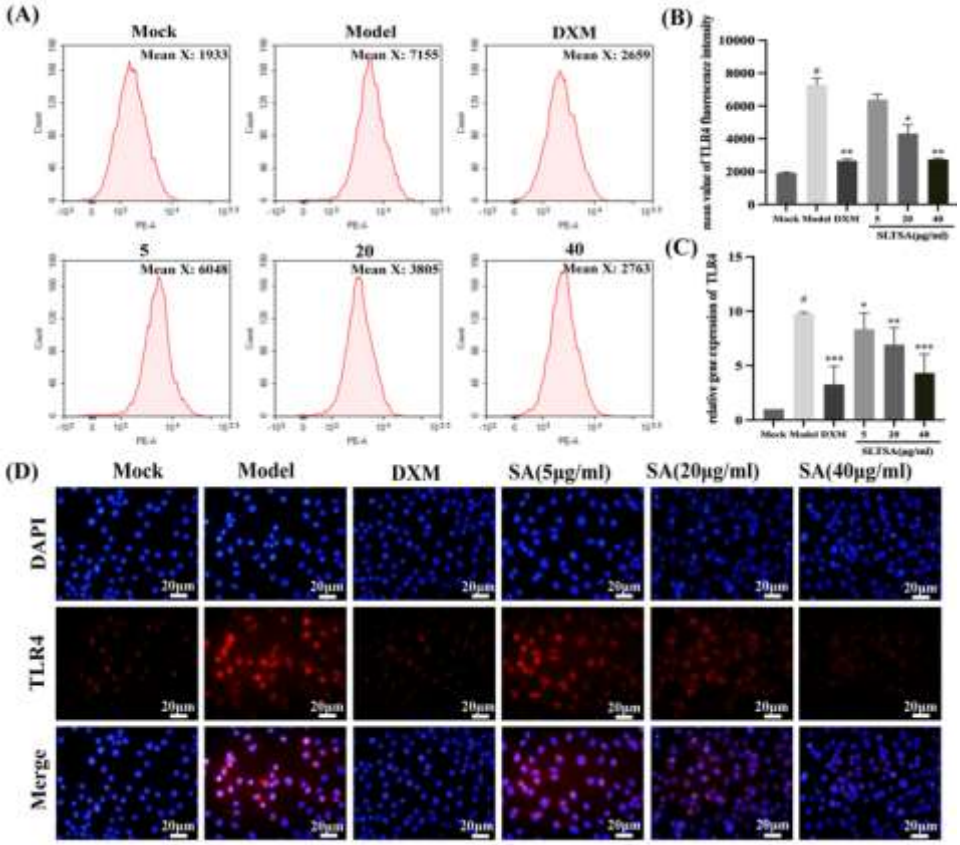

Fig. 5: Effect of SLTSA on TLR4 protein expression in RAW264.7 cells. (A) Flow cytometry results of TLR4 expression level. (B) Quantification of TLR4 expression level. (C) RT-qPCR results of the relative expression of TLR4 mRNA. (D) Cell immunofluorescence assay results of total cellular TLR4 protein expression. Scale bar = 20 μm Mock: diluent control group; Model: model group; DXM: dexamethasone control group; 5, 20, 40: three treatment groups with low, medium and high concentrations of SLTSA, respectively. #p<0.001 *vs.* Mock group, *p<0.05, **p<0.01 and ***p<0.001 *vs.* Model group.

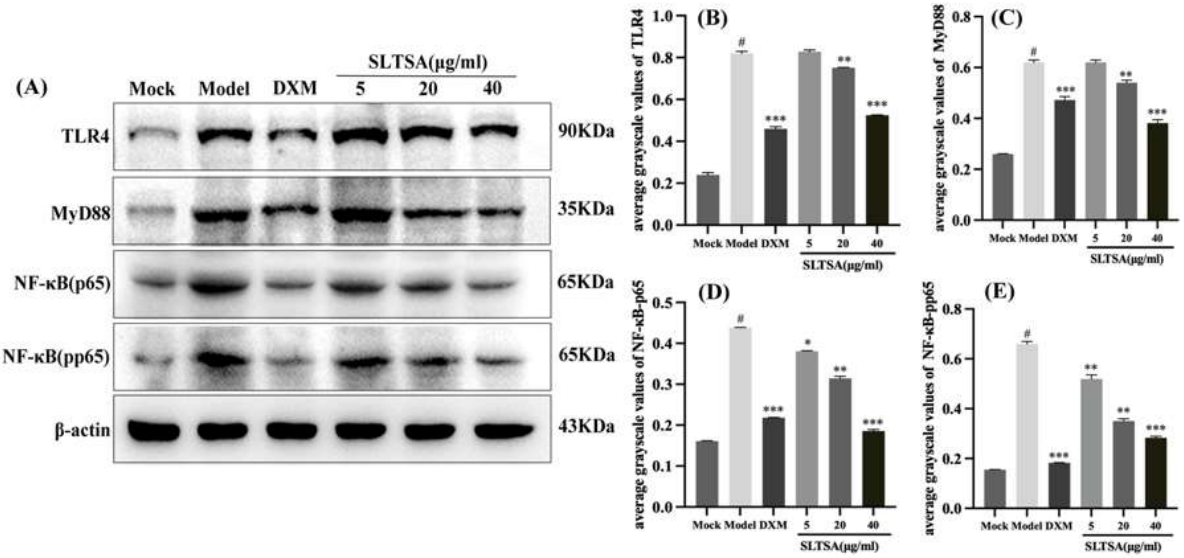

Fig. 6: Effect of SLTSA on the TLR4-MyD88-NF-κB inflammatory signaling pathway. (A) Western blot results. (B-E) Comparison of gray values of TLR4, MyD88, NF-κB p65 and NF-κB p65 phosphorylated protein in each group. Mock: diluent control group; Model: model group; DXM: dexamethasone control group; 5, 20, 40: three treatment groups with low, medium and high concentrations of SLTSA, respectively. #p<0.001 *vs.* Mock group, *p<0.05, **p<0.01 and ***p<0.001 *vs.* Model group.

Table 1: Primer pair sequences

Gene	Sequence 5'-3'
β-actin	Forward Primer: ATCACTATTGGCAACGAGCGGTTC
	Reverse Primer: CAGCACTGTGGGCATAGAGGTC
IL-1β	Forward Primer: GCAACTGTTCCTGAACTCAACT
	Reverse Primer: ATCTTTTGGGGTCCGTCAACT
IL-6	Forward Primer: CAGCAAGAGACTTCCATCCAG
	Reverse Primer: AGTGGTATAGACAGGTCTGTTGG
TNF-α	Forward Primer: CCCTCACACTCAGATCATCTTCT
	Reverse Primer: GCTACGACGTGGGCTACAG
TLR4	Forward Primer: ATGGCATGGCTTACACCACC
	Reverse Primer: GAGGCCAATTTTGTCTCCACA

Table 2: Results of animal experiments

Experimental parameters *in vivo*	Groups					
	Mock	Model	DXM	SLTSA 0.05mg	SLTSA 0.2mg	SLTSA 0.4mg
Ear swelling rate of mice (%)	——	91.60± 28.41	41.10± 10.80**	96.40± 15.71	64.00± 13.76*	41.70± 10.80**
Average dermal thickness of ear tissue (μm)	274.67± 24.25	1004.33± 181.59	491.67± 87.84***	963.00± 123.66	741.17± 29.46**	398.67± 84.18***
Leukocyte count in peritoneal fluid of mice ($\times10^4$/ml)	81.60± 9.84	140.38± 26.16	89.20± 13.52**	129.00± 22.19	106.20± 7.56*	95.00± 9.19**
Mouse serum ELISA IL-1β (pg/ml)	69.23± 7.61	133.44± 9.43	99.37± 5.53***	120.31± 4.07*	113.29± 4.60**	100.51± 4.63***
Mouse serum ELISA IL-6 (pg/ml)	101.00± 2.70	146.00± 2.19	111.24± 2.52***	140.56± 3.64*	127.38± 4.98**	112.18± 4.01***
Mouse serum ELISA TNF-α (pg/ml)	204.50± 10.38	502.40± 6.98	300.00± 10.80***	483.44± 22.09*	403.63± 16.54**	314.30± 3.50***

Mean ± SD values within two groups are significantly different, *p<0.05, **p<0.01 and ***p<0.001 *vs.* the Model group.

Table 3: Results of cell experiments

Experimental parameters *in vitro*	Groups					
	Mock	Model	DXM	SLTSA 5μg/ml	SLTSA 20μg/ml	SLTSA 40μg/ml
Cell viability (%)	100	——	——	99.24± 0.34	98.00± 1.73	97.40± 1.52
Cell ELISA IL-1β (pg/ml)	41.22± 2.95	84.15± 2.23	53.54± 1.60***	80.33± 1.47*	67.18± 1.59**	58.66± 3.17***
Cell ELISA IL-6 (pg/ml)	50.68± 2.98	79.36± 3.13	59.82± 2.80***	76.00± 3.00*	66.78± 3.03**	58.68± 2.94***
Cell ELISA TNF-α (pg/ml)	104.79± 4.83	228.83± 5.35	147.83± 4.22***	218.56± 8.78*	173.56± 3.75**	150.00± 4.06***
Relative gene expression of IL-1β	1	9.61± 0.26	3.97± 0.75***	9.12± 0.28*	8.08± 0.73**	5.84± 0.95***
Relative gene expression of IL- 6	1	16.85± 0.60	10.42± 0.70***	15.81± 0.73*	12.38± 2.57**	11.07± 2.04***
Relative gene expression of TNF- α	1	39.64± 0.33	19.81± 2.48***	33.25± 4.94*	32.57± 5.06**	22.14± 2.94***
Relative gene expression of TLR4	1	9.77± 0.13	3.28± 1.65***	8.35± 1.51*	6.93± 1.57**	4.32± 1.73***

Mean ± SD values within two groups are significantly different, *p<0.05, **p<0.01 and ***p<0.001 *vs.* the Model group.

Inhibition of acute abdominal inflammation in mice by SLTSA

To further demonstrate the anti-inflammatory effect of SLTSA *in vivo*, we performed the acute abdominal inflammation model in mice induced by thioglycolate broth and used cell counting to detect the number of leukocytes in the peritoneal fluid of mice and ELISA kits to measure the levels of pro-inflammatory cytokines in mice serum.

The results of the acute abdominal inflammation model in mice showed that the peritoneal fluid leukocyte count was significantly higher in the model group than in the Mock group (#p<0.001). After treatment with SLTSA, the leukocyte count was significantly reduced in all groups, and the most significant reduction was observed in the high concentration group (fig. 3 A, table 2). The ELISA results revealed that release of IL-1β, IL-6 and TNF-α in the serum of SLTSA-treated mice was significantly decreased compared with that in the model group, all differences were statistically significant (*p<0.05, **p<0.01 and ***p<0.001) (fig. 3 B-D, table 2).

These results suggested that SLTSA can reduce the peritoneal fluid leukocyte count and decrease the expression of inflammatory cytokines in mouse serum in a dose-dependent manner.

Inhibition of the expression of cellular pro-inflammatory cytokines by SLTSA

To clarify whether SLTSA was toxic to RAW264.7 cells, we examined the effect of three concentrations of SLTSA on cell viability with LPS for 24h by using CCK8 kits. Our data showed that none of the three concentrations of SLTSA damaged cell viability and the differences between each groups of SLTSA were not statistically significant compared with the Mock group (p>0.05), indicating that none of the drug concentrations exhibited significant cytotoxicity (fig. 4 A, table 3).

To investigate the anti-inflammatory effect of SLTSA, we detected the secretion of IL-1β, IL-6 and TNF-α cytokines by ELISA kits after stimulation with LPS. Our data showed that the secretion of all three cellular inflammatory cytokines in the Model group cells were significantly increased after stimulation with LPS compared to that in the Mock group (#p<0.001). Each SLTSA concentration treatment group could also significantly inhibited the secretion of inflammatory cytokines, and the effect of a high concentration of SLTSA was the most significant, and the differences were all statistically significant compared with the Model group (*p<0.05, **p<0.01 and ***p<0.001) (fig. 4 B-D, table 3).

To further investigate the anti-inflammatory effects of SLTSA *in vitro*, the gene expression of the cellular pro-inflammatory cytokines IL-1β, IL-6 and TNF-α was detected by RT-qPCR. Our data showed that, compared with the Mock group, the relative gene expression of the three inflammatory cytokines was significantly increased in the Model group after LPS stimulation (#p<0.001). The expression of inflammatory cytokines was significantly inhibited in each SLTSA treatment group, and the effect of a high concentration of SLTSA was the most significant; the differences were all statistically significant compared to the model group (*p<0.05, **p<0.01, ***p<0.001) (fig. 4 E-G, table 3).

These results indicated that SLTSA has an inhibitory effect on the expression and secretion of the three cellular inflammatory cytokines in a concentration-dependent manner.

Inhibition of TLR4 expression in RAW264.7 cells by SLTSA

To explore the anti-inflammatory target of SLTSA, we performed the RAW264.7 cellular inflammation model using LPS and then TLR4 protein and gene expression were examined using flow cytometry, immunofluorescence microscopy and RT-qPCR.

Flow cytometry results showed that compared with the Mock group, the wave peaks of the Model group as a whole shifted to the right, and the mean value also increased to more than triple, indicating that TLR4 protein expression on the cell membrane increased significantly after LPS stimulation. The wave peaks of the dexamethasone treatment group as a whole shifted to the left, and the mean value decreased significantly, while the wave peaks of the group treated with three different concentrations of SLTSA gradually shifted to the left, and the value decreased significantly (fig. 5 A). Fluorescence intensity decreased with increasing SLTSA concentration, indicating that SLTSA decreased TLR4 expression in a concentration-dependent manner (fig. 5 B).

RT–qPCR results showed that the relative expression of TLR4 in the Model group was significantly higher than that in the Mock group (#p<0.001), and after treatment with SLTSA, TLR4 gene expression in the medium and high concentration groups cells was significantly reduced (*p<0.05, **p<0.01), indicating that SLTSA could effectively inhibit the gene expression of TLR4 (fig. 5 C, table 3).

Cellular immunofluorescence assay results showed that the red fluorescence of cells in the Mock group was weak, the red fluorescence of cells in the Model group became stronger while the fluorescence became weaker as the concentration of SLTSA increased (fig. 5 D). These results indicated that SLTSA had a significant inhibitory effect on TLR4 expression.

Inhibition of TLR4/MyD88/NF-κB inflammatory signaling pathway activation by SLTSA

Given that TLR4/MyD88/NF-κB is a classical inflammatory signaling pathway, to demonstrate the anti-inflammatory mechanism of SLTSA, we detected the protein expression of the TLR4/MyD88/NF-κB cell signaling pathway by western blot. The results showed that this signaling pathway was significantly activated after LPS stimulation, the expression of TLR4 and MyD88 were significantly inhibited by medium and high concentrations of SLTSA, and the differences in grayscale values were statistically significant compared with the model group (fig. 6 A-C $^{**}p<0.01$, $^{***}p<0.001$). Similarly, the expression of NF-κB p65 and NF-κB pp65 was also inhibited by SLTSA in a concentration-dependent manner, and the differences in grayscale values were statistically significant compared to the model group (fig. 6 A, D, E $^{*}p<0.05$, $^{**}p<0.01$ and $^{***}p<0.001$).

These results demonstrated that SLTSA exerted anti-inflammatory effects by inhibiting the TLR4/MyD88/NF-κB signaling pathway.

DISCUSSION

As a traditional and natural Chinese herbal medicine, the extracts of SLT have been evaluated by acute and subchronic toxicity tests, showing low toxicity and high safety (Guo *et al.*, 2022), there has been great prospect in its pharmacological studies. In recent years, the anti-inflammatory activity of SLT has gradually received attention, and the effects of its different components have been explored (Zou *et al.*, 2023), however, the anti-inflammatory effects of SLTSA and its potential molecular mechanisms of action remain unknown. The results of this study fill the blank of the past research.

Inflammatory response is a common feature in almost all pathological conditions. Excessive inflammatory response causes additional disease deterioration and damage to organisms. With the rapid development of medical technology, an increasing number of synthetic drugs have been widely used to treat inflammation, but they are limited by their obvious adverse effects, including allergic reactions and renal impairment (Prete *et al.*, 2021; Min *et al.*, 2022). Consequently, the exploitation of natural and safe Chinese herbal medicine to suppress inflammation has long been a routine strategy. Animal inflammation models are effective and direct ways to understand the effects of drugs on inflammation in the body (Pavlou *et al.*, 2017; Said *et al.*, 2023), so we performed mice ear edema and acute abdominal inflammation model, and found that SLTSA has significant anti-inflammatory effects *in vivo.*

As an important characterization of the inflammatory response, the release of inflammatory cytokines is a key indicator for evaluating the degree of inflammatory development (Tan *et al.*, 2018), thus, we examined the secretion of inflammatory cytokines, including IL-1β, IL-6 and TNF-α, as important evidence that SLTSA is effective in exerting anti-inflammatory effects. Notably, the CCK8 assay was performed to confirm that SLTSA reduced inflammatory cytokines without affecting cell viability, which demonstrated that SLTSA can safely exert anti-inflammatory effects, confirming the natural low toxicity and side effects of SLTSA derived from traditional Chinese herbal medicine.

The TLR4/MyD88/NF-κB signaling pathway is not only an important subject for studying the pathogenesis of inflammation but also is a major component in exploring the mechanism of action of various drugs. Numerous studies have indicated the anti-inflammatory effects of Chinese herbal with this signaling pathway as the main molecular mechanism (Dai *et al.*, 2023; Li *et al.*, 2023). Our results showed that SLTSA exerts anti-inflammatory effects *in vitro* by inhibiting the activation of TLR4 and its downstream signaling pathway, although it is not clear whether SLTSA directly inhibits multiple proteins in this signaling pathway.

In addition, this study had some limitations. Firstly, there is insufficient evidence for the correlation between the two acute short-term inflammatory models in mice and the TLR4 signaling pathway, which means that the anti-inflammatory mechanism of SLTSA *in vivo* is still unclear and requires further research. Secondly, although the LPS is acknowledged as a major inflammatory model activator, the stimulation of LPS cannot completely imitate the complicated pathological inflammatory environments in patients. Finally, human studies for efficacy and safety is must before the SLTSA under test claimed to be effective in treating inflammation in human patients, suggesting that there are still considerable challenges to overcome in the transformation from experimental theory to clinical application.

Nevertheless, in this study, we determined that SLTSA has certain anti-inflammatory effects *in vivo* and can exert anti-inflammatory effects *in vitro* by inhibiting the TLR4/MyD88/NF-κB signaling pathway. As mentioned above, we believe that SLTSA has excellent prospects for anti-inflammatory research and our study provided essential evidence for the further development and utilization of SLT as a promising Chinese herbal medicine for the treatment of inflammation.

CONCLUSION

SLTSA has significant anti-inflammatory effects *in vivo* and *vitro* by inhibiting the TLR4/MyD88/NF-κB signaling pathway. These findings provided valuable insights into the potential application of SLTSA as anti-inflammatory agents.

REFERENCES

Allgaier R, Kandulski A, Gulow K, Maier L, Müller M and Tews HC (2023). Case report: Simultaneously induced neutropenia and hemolysis after a single metamizole dose. *Drugs RD.*, **23**(2): 93-98.

Bowman JD, Surani S and Horseman MA (2017). Endotoxin, toll-like receptor-4 and atherosclerotic heart disease. *Curr. Cardiol. Rev.*, **13**(2): 86-93.

Chen H, Chen H, Du K, Sun YJ, Hao ZY, Zhang YL, Bai J, Wang QH, Hu HY and Feng WS (2020). Solanrubiellin A: A hydroanthraquinone dimer with antibacterial and cytotoxic activity from *Solanum lyratum*. *Nat. Prod. Res.*, **34**(22): 3176-3181.

Christaki E, Marcou M and Tofarides A (2020). Antimicrobial resistance in bacteria: Mechanisms, evolution and persistence. *J. Mol. Evol.*, **88**(1): 26-40.

Ciesielska A, Matyjek M and Kwiatkowska K (2021). TLR4 and CD14 trafficking and its influence on LPS-induced pro-inflammatory signaling. *Cell Mol. Life Sci*., **78**(4): 1233-1261.

Dai Y, Lu Q, Li P, Zhu J, Jiang J, Zhao T, Hu Y, Ding K and Zhao M (2023). Xianglian Pill attenuates ulcerative colitis through TLR4/MyD88/NF-κB signaling pathway. *J. Ethnopharmacol*., **300**: 115690.

Dumlu FA, Aydin T, Odabasoglu F, Berktas OA, Kutlu Z, Erol HS, Halici MB, Cadirci E and Cakir A (2019). Anti-inflammatory and antioxidant properties of jervine, a sterodial alkaloid from rhizomes of *Veratrum album*. *Phytomedicine.*, **55**: 191-199.

Geng P, Xu X and Gao Z (2021). Sinomenine suppress the vitamin d3 and high fat induced atherosclerosis in rats via suppress of oxidative stress and inflammation. *J Oleo Sci*., **70**(12): 1815-1828.

Guo X, Weng L, Yi L and Geng D (2022). Toxicological safety evaluation in acute and 21-day studies of ethanol extract from *Solanum lyratum* Thunb. *Evid. Based Complement. Alternat. Med*., **2022**: 8518324.

Jin S, Nepal N and Gao Y (2022). The role of toll-like receptors in peptic ulcer disease. *Immunol. Med.*, **45**(2): 69-78.

Li B, Wang M, Chen S, Li M, Zeng J, Wu S, Tu Y, Li Y, Zhang R, Huang F and Tong X (2022). Baicalin mitigates the neuroinflammation through the TLR4/MyD88/NF-κB and MAPK pathways in LPS-stimulated BV-2 microglia. *Biomed. Res. Int*., **2022**: 3263446.

Li H, Zhang H and Zhao H (2023). Apigenin attenuates inflammatory response in allergic rhinitis mice by inhibiting the TLR4/MyD88/NF-κB signaling pathway. *Environ Toxicol.*, **38**(2): 253-265.

Li J, Tang W, Yang Y, Shen Q, Yu Y, Wang X, Fu Y and Li C (2021). A programmed cell-mimicking nanoparticle driven by potato alkaloid for targeted cancer chemoimmunotherapy. *Adv. Healthc. Mater*., **10**(13): e2100311.

Li JY, Wu SF, An YL, Yao CL, Yao S, Huang Y, Wei WL, Zhang JQ, Bi QR, Qu H and Guo DA (2023). Undescribed steroidal alkaloids from the bulbs of Fritillaria sinica. *Phytochemistry*, **213**: 113768.

Liang J, Liang W, Chen X and Wang Q (2022). Antibacterial sesquiterpenoids from *Solanum lyratum*. *Nat Prod Res.*, **36**(22): 5863-5867.

Liu X, Wang F, Chen Y, An Y, Cheng L, Wang L, Kong D, Zhao W, Tian J, Niu Y, Cui W, Zhang W, Xu Y, Ba Y and Zhou H (2023). Research progress on chemical components and pharmacological action of *Solanum lyratum* Thunb. *J. Pharm. Pharmacol*., **75**(3): 328-362.

Min HK, Kim SH, Kim HR and Lee SH (2022). Therapeutic Utility and Adverse Effects of Biologic Disease-Modifying Anti-Rheumatic Drugs in Inflammatory Arthritis. *Int. J. Mol. Sci*., **23**(22): 13913.

Mohammad S and Thiemermann C (2020). Role of metabolic endotoxemia in systemic inflammation and potential interventions. *Front. Immunol.*, **11**: 594150.

Pavlou S, Wang L, Xu H and Chen M (2017). Higher phagocytic activity of thioglycollate-elicited peritoneal macrophages is related to metabolic status of the cells. *J. Inflamm. (Lond).*, **14**: 4.

Prete A and Bancos I (2021). Glucocorticoid induced adrenal insufficiency. *BMJ*., **374**: n1380.

Said K, Hamayun M, Rauf M, Khan SA, Arif M, Alrefaei AF, Almutairi MH and Ali S (2023). Simultaneous study of analysis of anti-inflammatory potential of *Dryopteris ramosa* (C. Hope) C. Chr. using GC-mass and computational modeling on the xylene-induced ear oedema in mouse model. *Curr. Pharm. Des*., **29**(41): 3324-3339.

Shen HR, Xu X and Li XL (2021). Berberine exerts a protective effect on rats with polycystic ovary syndrome by inhibiting the inflammatory response and cell apoptosis. *Reprod Biol Endocrinol*., **19**(1):3.

Tam JSY, Coller JK, Prestidge CA and Bowen JM (2023). Investigation of TLR4 antagonists for prevention of intestinal inflammation. *Inflammation*, **46**(1): 103-114.

Tan J, Deng Z, Liu G, Hu J and Liu S (2018). Anti-inflammatory polymersomes of redox-responsive polyprodrug amphiphiles with inflammation-triggered indomethacin release characteristics. *Biomaterials*, **178**: 608-619.

Tasneem S, Liu B, Li B, Choudhary MI and Wang W (2019). Molecular pharmacology of inflammation: Medicinal plants as anti-inflammatory agents. *Pharmacol Res*., **139**: 126-140.

Wang Y, Sadike D, Huang B, Li P, Wu Q, Jiang N, Fang Y, Song G, Xu L, Wang W and Xie M (2023). Regulatory T cells alleviate myelinloss and cognitive dysfunction by regulating neuroinflammation and microglial pyroptosis via TLR4/MyD88/NF-κB pathway in LPC-induced demyelination. *J. Neuroinflammation*, **20**(1): 41.

Xu D, Zhao W, Feng Y, Wen X, Liu H and Ping J (2022). Pentoxifylline attenuates nonalcoholic fatty liver by

inhibiting hepatic macrophage polarization to the M1 phenotype. *Phytomedicine*, **106**: 154368.

Xu YL, Lv J, Wang WF, Liu Y, Xu YJ and Xu TH (2018). New steroidal alkaloid and furostanol glycosides isolated from Solanum lyratum with cytotoxicity. *Chin J. Nat Med*., **16**(7): 499-504.

Zhang B, Zeng M, Li M, Kan Y, Li B, Xu R, Wu Y, Wang S, Zheng X and Feng W (2019). Protopine protects mice against LPS-iInduced acute kidney injury by inhibiting apoptosis and inflammation via the TLR4 signaling pathway. *Molecules*, **25**(1):15.

Zhang C, Li Z, Wang J, Jiang X, Xia M, Wang J, Lu S, Li S and Wang H (2021). Ethanol extracts of *Solanum lyratum* Thunb. regulate ovarian cancer cell proliferation, apoptosis and epithelial-to-mesenchymal transition (EMT) via the ROS-mediated p53 pathway. *J. Immunol Res*., 5569354.

Zhang DW, Li GH, Yu QY and Dai SJ (2010). New anti-inflammatory 4-hydroxyisoflavans from *Solanum lyratum*. *Chem. Pharm. Bull. (Tokyo)*, **58**(6): 840-842.

Zhang J, Mi Y, Zhou R, Liu Z, Huang B, Guo R, Wang P, Lu Y, Zhou Y and Quan S (2020). The TLR4-MyD88-NF-κB pathway is involved in sIgA-mediated IgA nephropathy. *J. Nephrol.*, **33**(6): 1251-1261.

Zhao L, Wang L, Di SN, Xu Q, Ren QC, Chen SZ, Huang N, Jia D and Shen XF (2018). Steroidal alkaloid solanine A from *Solanum nigrum* Linn. exhibits anti-inflammatory activity in lipopolysaccharide/interferon γ-activated murine macrophages and animal models of inflammation. *Biomed. Pharmacother.*, **105**: 606-615.

Zhao Y, Gao WK, Wang XD, Zhang LH, Yu HY and Wu HH (2022). Phytochemical and pharmacological studies on *Solanum lyratum*: A review. *Nat. Prod. Bioprospect*., **12**(1): 39.

Zhou ZS, Zhao YL, Hu BY, Wang B, Liu YP, Zhu YY, He YJ, Wang ZJ, Dai Z, Zhao LX and Luo XD (2023). Steroidal alkaloid with unprecedented triheterocyclic architecture. *Chem. Commun. (Camb)*, **59**(3): 326-329.

Zou C, Liu L, Huang C and Hu S (2022). Baiying qingmai formulation ameliorates thromboangiitis obliterans by inhibiting HMGB1/RAGE/NF-κB signaling pathways. *Front. Pharmacol*., **13**: 1018438.

Zou D, Li X, Zhou X, Luo B, Faruque MO, Hu S, Chen J and Hu X (2023). The interaction of anti-inflammatory and anti-tumor components in the traditional Chinese medicine *Solanum lyratum* Thunb. *Nat. Prod. Res*., **16**: 1-5.